Applied Surface Science 257 (2011) 4575–4580

Contents lists available at ScienceDirect

Applied Surface Science

journal homepage: www.elsevier.com/locate/apsusc

Bioactive coating on titanium implants modified by Nd:YVO_4 laser

Edson de Almeida Filho[a,*], Alexandre F. Fraga[b], Rafael A. Bini[a], Antonio C. Guastaldi[a]

[a] Universidade Estadual Paulista – UNESP, Instituto de Química, Grupo de Biomateriais, Caixa Postal 355, 14800-900, Araraquara, SP, Brazil
[b] Universidade Federal de São Carlos – UFSCar- Departamento de Engenharia de Materiais-DEMa Rodovia Washington Luís, km 235 - SP-310 13565-905, São Carlos, SP, Brazil

ARTICLE INFO

Article history:
Received 24 June 2010
Received in revised form 6 December 2010
Accepted 12 December 2010
Available online 17 December 2010

Keywords:
Laser ablation
Apatites
Titanium
Biomimetic method

ABSTRACT

Apatite coating was applied on titanium surfaces modified by Nd:YVO_4 laser ablations with different energy densities (fluency) at ambient pressure and atmosphere. The apatites were deposited by biomimetic method using a simulated body fluid solution that simulates the salt concentration of bodily fluids. The titanium surfaces submitted to the fast melting and solidification processes (ablation) were immersed in the simulated body fluid solution for four days. The samples were divided into two groups, one underwent heat treatment at 600 °C and the other dried at 37 °C. For the samples treated thermally the diffractograms showed the formation of a phase mixture, with the presence of the hydroxyapatite, tricalcium phosphate, calcium deficient hydroxyapatite, carbonated hydroxyapatite and octacalcium phosphate phases. For the samples dried only the formation of the octacalcium phosphate and hydroxyapatite phases was verified. The infrared spectra show bands relative to chemical bonds confirmed by the diffraction analyses. The coating of both the samples with and without heat treatment present dense morphology and made up of a clustering of spherical particles ranging from 5 to 20 μm. Based on the results we infer that the modification of implant surfaces employing laser ablations leads to the formation of oxides that help the formation of hydroxyapatite without the need of a heat treatment.

1. Introduction

Dental implants represent a treatment alternative for buccal rehabilitation, that is used in various clinical situations with high predictability of success due to the bone integration [1,2]. This process depends on several factors, among which is the macroscopic and microscopic quality of the implant surface that interferes in the establishment of the adequate bone/implant interaction and in this interface strength [3].

Titanium implant surface treatments have been proposed to improve the physical–chemical and morphological properties to improve the bone quality and quantity on the bone/implant interface [4]. These treatments can speed up the bone repair around implants, which can benefit the bone integration process in areas of low bone density, in clinical situations of immediate charge or early charge [5]. Investigations found that implants with rough morphology surface present better bone repair results when compared with machined surface implants [6–8]. The likely factors are related to the best remodeling activity on the bone/implant interface observed in implants with rough morphology. This generates an increase of retention of blood clot, of the area of implant/tissue surface and the cellular migration and proliferation [9–16].

The alteration of implant surface by laser ablation irradiation was originally introduced in the materials engineering [17]. This process results in modifications in the surface microstructure with an increase in the specific area, in resistance to corrosion and in the biocompatibility of the titanium [18]. Besides producing a complex surface morphology with a high degree of purity, this method also has the characteristic of being a controllable and reproducible process [10,19].

Implant surfaces with bioactive materials benefit the interaction between bone tissues and implant by means of the biologically active apatite layer similar to the bone tissue [20,21]. The hydroxyapatite (HA, $[Ca_{10}(PO_4)_6(OH)_2]$) belongs to the calcium phosphate system and is present in bones and teeth of all vertebrates. The hydroxyapatite represents 5% of the total weight of an adult individual, 55% of the bone composition, 96% of the tooth enamel composition and 70% of the dentine. In living organisms, the ease of cationic and anionic replacement leads the HA to act as a calcium and phosphorus reserve and as a regulating system of different ions in the body liquids by means of its release or storage [22].

These properties enable the hydroxyapatite to be used to recover metallic implants to combine the mechanic property advantages of the metals with its excellent biocompatibility and bioactivity, thus providing the increase of the implant interface interaction with the bone tissue [23,24].

* Corresponding author.
E-mail address: edsonafilho@yahoo.com.br (E.d.A. Filho).

0169-4332/$ – see front matter © 2010 Elsevier B.V. All rights reserved.
doi:10.1016/j.apsusc.2010.12.056

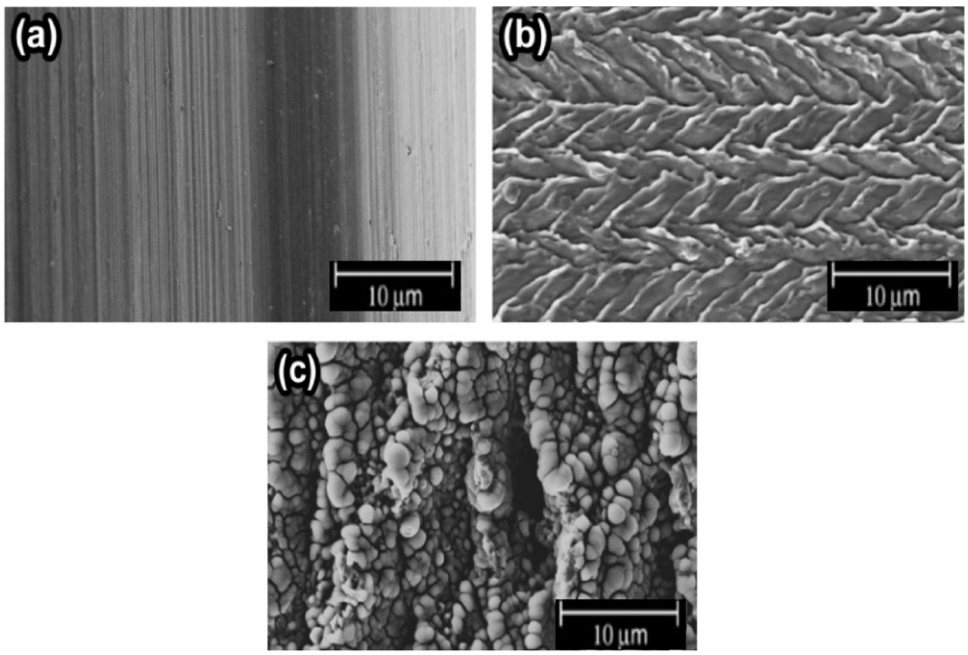

Fig. 1. SEM of the c.p. Ti (a) and after laser ablation (b) F56 and (c) F280.

In 1990 Abe and collaborators developed a method that allows coating practically any substract with a uniform layer of HA similar to the biologic one, named Biomimetic Method of Coating [25]. The major advantages of this technique include the possibility of controlling the settled layer thickness, the increase of adhesion to the metallic substrate and the surface morphology that increases the host response to the implant, benefiting the bone integration in shorter time periods [25,26].

Nowadays, the researches in the dental implant area establish a suitable interface for the settling process of bioactive materials. The irradiation by laser ablation as a method of modification of surface has been studied with the intention of improving the metal/ceramics interface. In view of this, in the present work calcium phosphate ceramics were deposited on titanium surfaces modified by Nd:YVO_4 laser ablation.

2. Experimental

2.1. Surface modification by laser

The c.p. Ti samples ($10 \times 10 \times 2$ mm) were submitted to irradiation by multipulse laser Nd:YAG Digilaser DML 100 ($\lambda = 1064$ nm). The surfaces were modified, at ambient pressure and atmosphere, with fluencies (high speed melting and solidification process) of 56 and 280 J cm^{-2} (F56 and F280), respectively. The laser parameters were configured according to the procedure proposed by Braga [16]. After the irradiations, the samples were submitted to ultrasonically washed ethylic alcohol solutions, of acetone and distilled water separately, then were dried in oven and placed in NaOH solution (5 mol L^{-1}) for a period of 24 h, at 60 °C.

2.2. Sample coating by biomimetic method

The irradiated samples were immersed in a 1.5 SBF solution and pH 7.25 and stayed in oven during four days at 37 °C. The 1.5 SBF solution was changed every 24 h during the coating period. Table 1 shows the ionic concentrations of the SBF solution [27,28].

After the coating process by the biomimetic method, the samples were submitted to heat treatment. The samples were divided into two groups: G1 for the samples dried in oven at 37 °C (Ti/AP, F56/AP and F280/AP), and G2 for the samples treated thermally at 600 °C for a period of 1 h, with the heating rate of 5 °C/min, both for the heating and the cooling (Ti/AP, F56/AP-TT and F280/AP-TT). All heat treatments were made in ambient atmosphere and pressure.

3. Characterization

The scanning electron microscopy (SEM) was made using a LEO microscope, model 440, coupled to a Si (Li) energy dispersive analyzer with Be window, model 760 and 133 eV spectroscopic resolution by dispersive energy – EDS. The X-ray diffraction analyses were made on a Siemens D5000 X-ray diffractometer, angular scanning 20–60° with 0.02 pitch (2θ), and the pitch time was 10 s for each sample, on the Bragg–Brentano build-up, using Cu (kα1) radiation. Surface roughness was measured for a Laser Microfocus Expert IV. The samples wettability was carried out in a Contact Angle System OCA 15 device (DataPhysics). For the chemical bond characterization of the apatite settlings, the technique used the vibrational spectroscopy in the infrared region that was performed in a FTIR Nicolet Magna 550 spectrophotometer with diffuse reflectance DRIFT Collector™.

4. Results and discussion

4.1. Surface irradiation by laser

The SEM micrographs of the surface modifications by laser beam obtained with different scanning velocities are displayed in Fig. 1. For a sample F280, it was produced a surface with

Table 1
Solution SBF used in the apatite coating.

	Ions (mmol L^{-1})							
	Na^+	K^+	Ca^{2+}	Mg^{2+}	HCO_3^{2-}	Cl^-	HPO_4^{2-}	SO_4^{2-}
Blood plasma	142.0	5.0	2.5	1.5	27.0	103.0	1.0	0.5
1.5 SBF	213.0	7.5	3.8	2.3	6.3	223.0	1.5	0.75

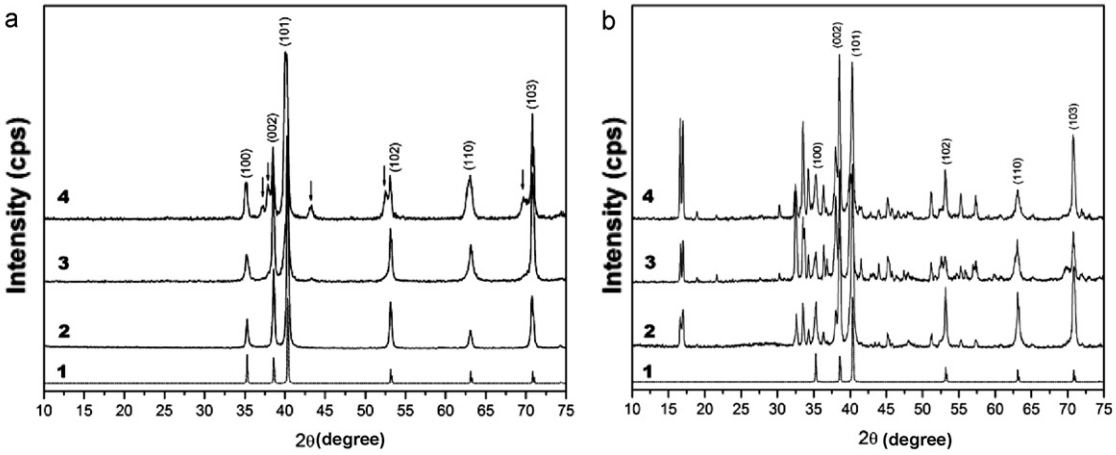

Fig. 2. X-ray spectra relative to samples after (a) laser ablation and (b) NaOH process. The numbers 1, 2, 3 and 4 represent the α-Ti pattern, c.p. Ti experimental, F56 and F280, respectively.

higher roughness than for sample F56. This morphology related to the highest energy density to provide the surface (fluency), producing a larger melted metal zone. When a metal surface is submitted by laser beam the ablation process can or may occur, which is directly correlated with energy density used. Ablation process is characterized by a quick melting (melted metal zone formation) and solidification process on metal surface [29].

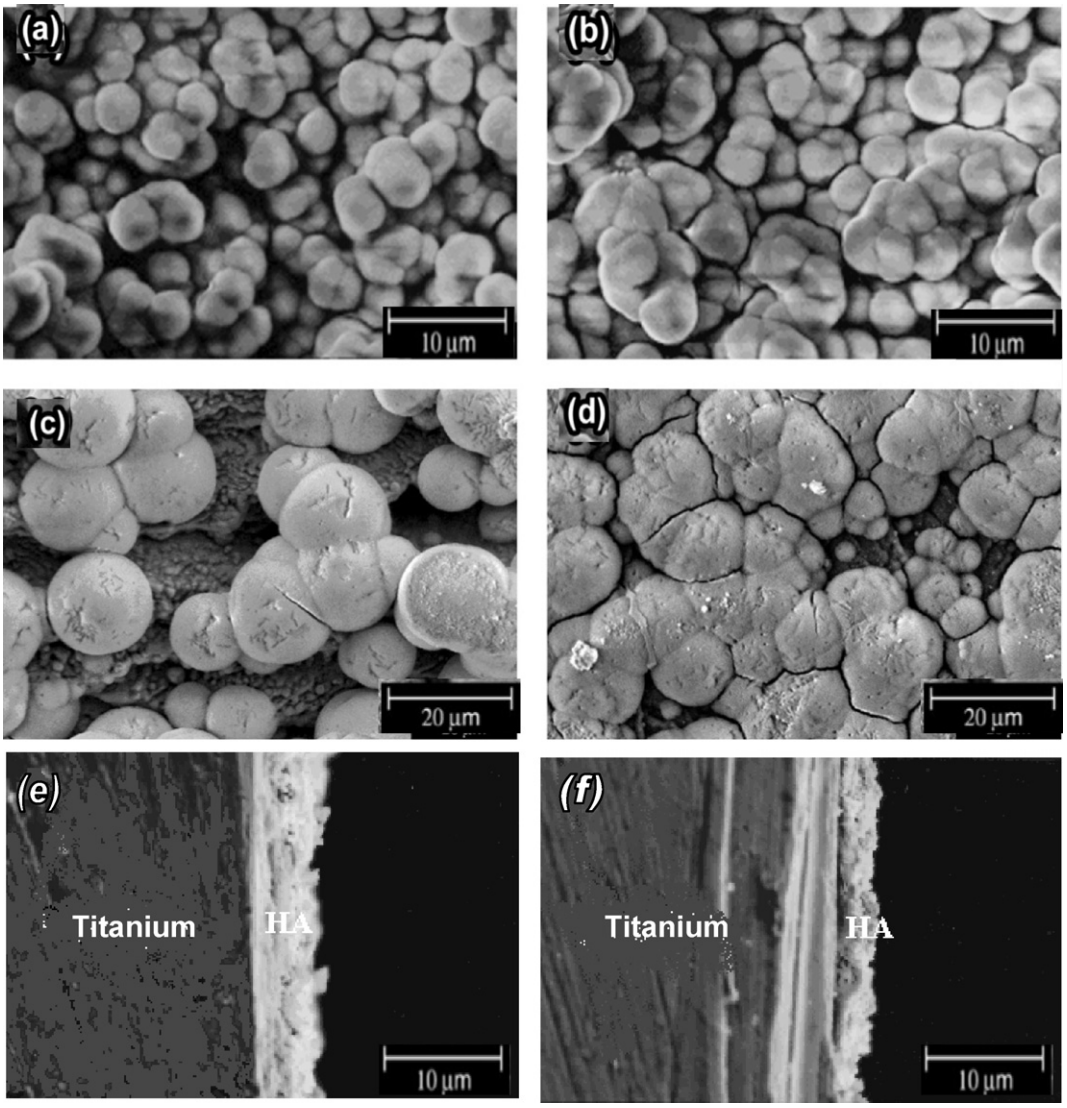

Fig. 3. SEM of the apatite coatings on surfaces modified by laser (a) F56/AP, (b) F280/AP, (c) F56/AP-TT and (d) F280/AP-TT. The cross sectional (e) F56/AP-TT and (f) F280/AP-TT.

Table 2
Surface roughness and contact angles (deg) of laser and cp Ti samples.

Surface	Average r.m.s. values (μm)	Contact angle (deg)
cp Ti	0.0072 ± 0.0013	4 ± 1.25
F56	0.6874 ± 0.2243	2 ± 0.15
F280	1.9760 ± 0.3781	0 ± 0.05

The melted metal zone created by ablation process can produce morphologies with different roughness degrees. Table 2 shows the surface roughness obtained by laser ablation. R.m.s. roughness measurements show that the fluency of 280 J cm^{-2} produced high roughness degree (1.9760 μm). The fluency of 56 J cm^{-2} it was obtained 0.6874 μm, whereas for the cp. Ti the r.m.s. roughness value was 0.0072 μm. This high roughness value for sample can be explained by the fivefold fluency instead of F56 sample. Roughness is an important characteristic for dental implants. In the literature it has also been noted that the cellular adhesion, the proliferation and detachment strength are sensitive to surface roughness [30]. Another important factor that contributes to better cell attachment is to obtain a hydrophilic surface [31]. All the samples were submitted to contact angle measures with distilled water, as shown in Table 2. For the F280 and F56 samples the values of zero and two degrees were obtained, while for cp. Ti the value of four degree was measured. These different wettability degrees indicate the formation of different compounds on titanium surface, which are produced by laser ablation.

XRD spectra of the cp. Ti before and after laser ablations are displayed in Fig. 2. All samples showed well-resolved (1 0 0), (0 0 2), (1 0 0), (1 0 2), (1 1 0) and (1 0 3) reflections, which are characteristic X-ray diffraction patterns of the α-phase titanium [32] (Fig. 2a). For samples submitted to laser ablation, the oxidation process was verified. For the F56 sample a small enlargement of diffraction patterns of small enlargement was observed, however, for the F280 sample new peaks at 37.3°, 37.8°, 43.2°, 52.5° and 69.7° were found. X-ray diffraction analyses showed the formation of TiO, Ti_3O and Ti_6O oxides, which are classified as oxygen-deficient non-stoichiometric oxides. In previous works Braga [12] and Bini [33] verified that the fast melting and solidification process of the metallic surface at ambient pressure and atmosphere lead to the build-up of different stoichiometric and non-stoichiometric titanium oxides. Titanium is able to absorb about 40% of atomic oxygen into its crystal lattice (~18% m/m) in solid interstitial solution [12,13]. Thus, the energy supplied by the laser benefits the diffusion of oxygen atoms into the α-Ti network. However, the fast solidification of the surface stabilizes the formation of these non-conventional phases [34,35].

Fig. 2(b) shows X-ray diffraction patterns of samples after sodium hydroxide treatment. Besides α-Ti diffraction patterns, a formation of a polycrystalline system was observed. Analyses made through JCPDS standards [32] indicated the stabilization of sodium titanium oxide with different stoichiometrics on metal surface. Referring picks to the sodium titanium oxide such as $NaTiO_2$ (#16-251), Na_2TiO_3 (#37-345), Na_4TiO_4 (#42-513), and $Na_{2.08}Ti_4O_9$ (#84-2047) were found through X-ray diffraction [32]. The formation of this polycrystalline system is an important step, according to Kokubo, the production of sodium titanium oxide on the surface may induce the formation of an active and favorable layer for the stabilization of the calcium phosphate system on the substrate surface [15].

Fig. 3 shows the apatite coating on the irradiated surfaces by laser beam and the NaOH process submitted. Micrographs showed the formation of clustering spherical particles, which are typically found according to the HAP phase. The spherical particle size ranged from 5 to 20 μm. The main difference is that the sample was observed when heat treatment was applied; F280/AP-TT and F56/AP-TT, Figs. 3(c) and (d), respectively. For the thermally treated samples, an increase in the particles produced by thermal diffusion was observed, which provided an increase in the crystallinity of the coating. That is in agreement with the data found in the literature [33–35]. For both samples after thermal treatment the coating thickness was around 10 μm (Fig. 3e and f). Thus, it was can be observed that so much morphology as thickness of calcium phosphate layer formed on the substrate did not suffer interference from surface roughness before settling. However, the new compounds formed by the laser beam influenced the stabilization of different apatite phases.

Fig. 4 shows the X-ray spectra relative to samples Ti/AP-TT, F280/AP-TT and F56/AP-TT. Inset at spectra are diffractogram samples without heat treatment (Ti/AP, F280/AP and F56/AP) and the HA and OCP patterns in 2θ region between 24° and 36°. For the

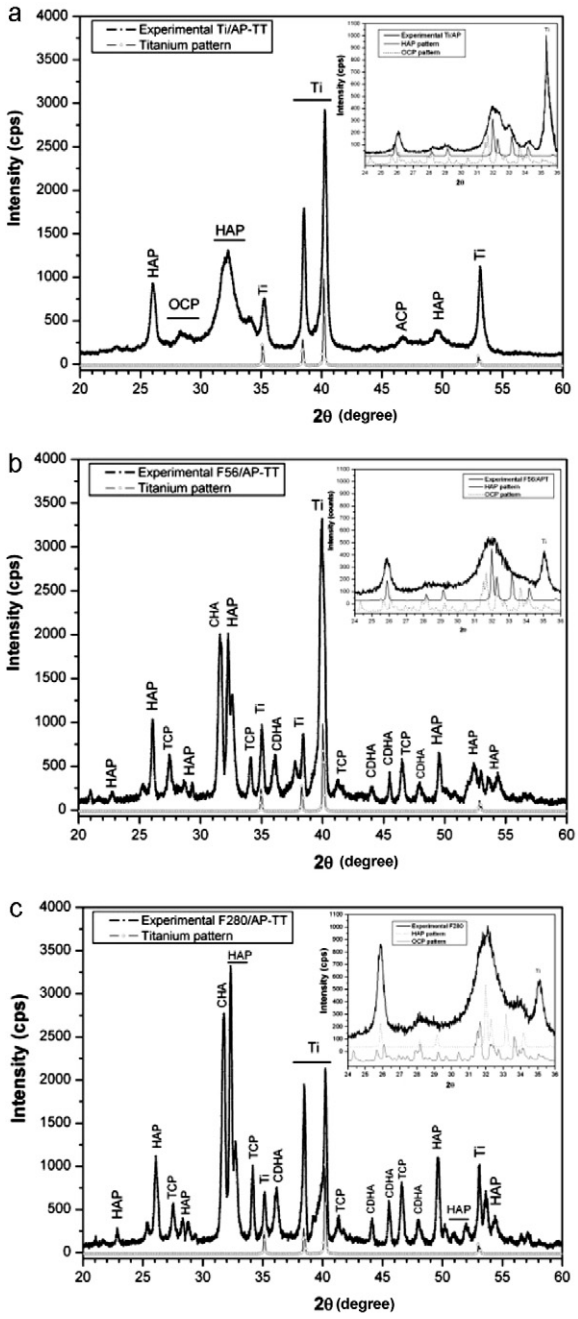

Fig. 4. X-ray spectra relative to samples (a) Ti/AP-TT, (b) F56/AP-TT and (c) F280/AP-TT.

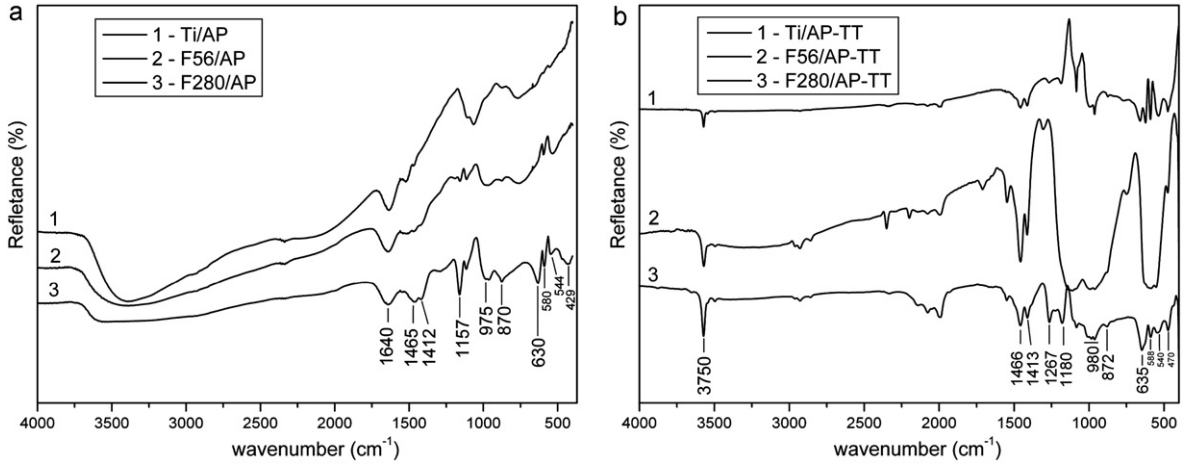

Fig. 5. Infrared spectra by diffuse reflectance of the samples (a) without and (b) with thermal treatment.

samples without heat treatment only the presence of the HA and OCP phases was verified. Table 3 shows three possible reactions of the calcium phosphate system [20,21,30]. According to Reaction (A.1) the ACP phase changes to the OCP phase via loss of calcium ions and hydroxyl transformation into hydration waters. In addition to Reaction (A.2), the OCP phase is one of the likely precursors of the hydroxyapatite phase [36]. Analyzing the characteristic peaks of phase HA, sample F280/AP showed more intensity than sample F56/AP. This difference is related to the different concentrations of non-stoichiometer oxides on the titanium surface. Bini et al. [33] quantified the concentrations of non-stoichiometric oxides formed by the Rietveld method, and was verified that as the fluency increases, the concentration of the oxides on the surface increases as well.

After the heat treatment, in addition to phases HA and OCP, the formation of the phases, beta tricalcium phosphate (β-TCP), calcium deficient HA (CDHA) and carbonated HA (CHA) was found. The solution used in the coating production was 1.5 SBF, which was modified by Herrera, collaborators of the solution were originally proposed by Kokubo [28,36]. The 1.5 SBF solution has higher calcium ion concentrations and lower bicarbonate ion concentrations than the Blood Plasma concentrations. This change was made to minimize the stabilization of the carbonated hydroxyapatite and calcium deficient phases. However, as verified in the diffractograms, after the heat treatment, the presence of the phases CDHA and CHA is observed. The CHA phase occurs when the CO_3^{2-} ions replace the PO_4^{3-} or the OH^- ions in the network. Analyzing the cell parameters between the JCPDS standards of the HA and CHA phases with the experimental data, the formation of the CHA phase of the type B [37–39] was observed. As the heat treatment was carried out at 600 °C, a percentage of the CHA phase may form both the HA phase and the β-TCP, according to Reaction (A.3) detailed in Table 3. Another possible source of formation of the β-TCP phase is the dehydration of the non-stoichiometric HA phase, according to Reaction (A.4).

Table 3
Phase transformations that may occur in the calcium phosphate system [40].

Calcium phosphate reactions
(A.1) ACP → OCP
$3Ca_3(PO_4)_2H_2O + 5H_2O + H_3O^+ \rightarrow Ca_8(HPO_4)_2(PO_4)_4.5H_2O + Ca^{2+} + OH^- + H_2O$
(A.2) OCP → HA
$Ca_8(HPO_4)_2(PO_4)_4.5H_2O + Ca^{2+} + OH^- + H_2O \rightarrow Ca_9(HPO_4)_2(PO_4)_4(OH)_2 + 4H_2O + H_3O^+$
$Ca_9(HPO_4)_2(PO_4)_4(OH)_2 + Ca^{2+} + OH^- + H_2O \rightarrow Ca_{10}(PO_4)_6(OH)_2 + H_2O + H_3O^+$
(A.3) CHA → CDHA
$Ca_{10-x}(HPO_4)_x(PO_4)_{6-x}(OH)_{2-x}nH_2O \xrightarrow{\Delta} Ca_{10-x}(P_2O_7)_x(PO_4)_{6-2x}(OH)_2 + nH_2O_{(g)}$
(A.4) CDHA → HA + β-TCP
$Ca_{10-x}(P_2O_7)_x(PO_4)_{6-2x}(OH)_2 + nH_2O_{(g)} \xrightarrow{\Delta} (1-x)Ca_{10}(PO_4)_6(OH)_2 + 3xCa_3(PO_4)_2 + xH_2O_{(g)}$

When the samples are submitted to the heat treatment above 600 °C (Fig. 5b), besides occurring the loss of the hydration water molecules, according to Aoki molecular rearrangement processes occur which provides changes in the apatite phases[36]. These processes can be observed in the infrared spectra of the F56/AP-TT and F280/AP-TT samples. The disappearance of a wide band in the 3000–3700 cm^{-1} region corresponding to the water molecule hydroxyl for the samples without heat treatment and the presence of an intense and narrow band relative to the hydroxyl of the HA phase were observed. Fig. 5(b) shows the spectra of samples F56/AP-TT and F280/AP-TT, in which the presence of the stretching out mode at 3750 cm^{-1} was observed. The presence of the three distinct modes in the 630, 1000–1200 and 3700 regions has been then observed with a signature of the HA phase [42–44]. The structural rearrangements provided by the thermal energy supplied to the system for the formation of the HA phase can also lead to the stabilization of other phases. According to Table 2, the CHA phase may undergo structural rearrangement to generate both the HA phase and the β-TCP phase, according to Reaction (A.3). As verified by the X-ray analysis, the CDHA phase may also undergo rearrangement and form the HA and β-TCP phases, according to Reaction (A.4).

Fig. 5 shows the infrared spectra for the samples with and without heat treatment, which phosphate group was observed in all samples due to the presence of the stretching out modes in 910–1220 cm^{-1} and deformation in 540–600 cm^{-1} [36–38]. The infrared analyses confirmed the formation of the type B CHA phase. The presence of the vibration modes in three distinct regions, 880, 1465 and 1412 cm^{-1}, indicate the formation of the type B CHA phase [39–41]. Fig. 5(a) shows the spectra of samples F56/AP and F280/AP. It is possible to observe the presence of the vibration mode of the hydroxyl in 630 cm^{-1} relative to HA phase. However, as the samples were only put in oven at 60 °C, a wide band in the 3000–3700 cm^{-1} region and one in the 1600–1650 cm^{-1} region that refer to the water molecule hydroxyls were found.

5. Conclusion

Based on the results, it can be inferred that the modification of implant surfaces employing laser ablation enables the formation

of oxides that help form HA without the need of a heat treatment. This procedure presents itself as promising as an implant surface modifier for being a clean, reproducible, economically feasible process and suitable for the deposition of bioactive coatings. However, after the heat treatment the formation of different phases of calcium phosphate (ACP, OCP and β-TCP) was observed. Further investigation is required for in vitro and in vivo studies.

Acknowledgments

The authors would like to thank CNPq and FAPESP for the financial support.

References

[1] H. Nakajima, T.T. Okabe, Titanium in dentistry: development and research in the U.S.A., J. Dent. Mater. 15 (1996) 77–90.
[2] Espident GmbH – Aesthetic dental products. Triceram® Triline Ti. Germany, 1999. (Información del producto y modo de empleo).
[3] B. Touati, P. Miara, D. Nathanson, Sistemas cerâmicos atuais, in: Odontologia estética e restaurações cerâmicas, São Paulo, Ed. Santos, 2000, pp. 25–37.
[4] M.G. Troia Junior, Avaliação da resistência de uma porcelana de baixa fusão em combinação com o titânio comercialmente puro e liga de titânio-alumínio-vanádio. Piracicaba, 2001. 92p. Tese (Mestrado em Clínica Odontológica, área de Prótese Dental) – Faculdade de Odontologia de Piracicaba, Universidade Estadual de Campinas.
[5] H. Kimura, C.J. Horning, M.I. Okazah, Oxidation effect on porcelain–titanium interface reaction and bond strength, J. Dent. Mat. 9 (1990) 91–99.
[6] T. Albrektsson, A. Wennerberg, Oral implant surfaces. Part 1. Review focusing on topographic and chemical properties of different surfaces and in vivo responses to them, Int. J. Prosthodont. 17 (2004) 536–543.
[7] F. Grizon, E. Aguado, G. Huré, M.F. Baslé, D. Chappard, Enhanced bone integration of implants with increased surface roughness: a long term study in the sheep, J. Dent. Mater. 30 (2002) 195–203.
[8] W. Zechner, L.S. Tang, G. Furst, Tepper, U. Thams, G. Mailath, G. Watzek, Osseous healing characteristics of three different implant types, Clin. Oral. Implants Res. 14 (2003) 150–157.
[9] D. Buser, T. Nydegger, H.P. Hirt, D.L. Cochran, L.P. Nolte, Removal torque values of titanium implants in the maxilla of miniature pigs, Int. J. Oral. Maxillofac. Implants. 13 (1998) 611–619.
[10] K. Gotfredsen, T. Berglundh, J. Lindhe, Bone reactions adjacent to titanium implants with different surface characteristics subjected to static load. A study in the dog (II), Clin. Oral. Implants Res. 12 (2001) 196–201.
[11] D. Buser, R. Mericske-Stern, J.P. Bernard, A. Behneke, N. Behneke, H.P. Hirt, U.C. Belser, N.P. Lang, Long-term evaluation of non-submerged TI implants. Part 1:8-year life table analysis of a prospective multi-center study with 2359 implants, Clin. Oral. Implants Res. 8 (1997) 161–172.
[12] F.J.C. Braga, R.F.C. Marques, E.A. Filho, A.C. Guastaldi, Surface modification of Ti dental implants by Nd:YVO_4 laser irradiation, Appl. Surf. Sci. 253 (2007) 9203–9208.
[13] A.H. Aparecida, M.V.L. Fook, M.L. Santos, A.C. Guastaldi, Influência dos íons K^+ e Mg^{2+} na obtenção de apatitas biomiméticas, Ecl. Quím. 30 (2005) 13–18.
[14] Y. Abe, T. Kokubo, T. Yamamuro, Apatite layering on ceramics, metals and polymers utilizing a biological process, J. Mater. Sci. Mater. Med. 1 (1990) 233–238.
[15] T. Kokubo, T.H. Takadama, How useful is SBF in predicting in vivo bone bioactivity? Biomaterials 27 (2006) 2907–2915.
[16] J. Nogueras-Bayona, F.J. Gil, J. Salsench, J. Martinez-Gomis, Roughness and bonding strength of bioactive apatite layer on dental implants, Implant. Dent. 13 (2004) 185–189.
[17] H.W. Kim, Y.H. Koh, L.H. Li, S. Lee, H.E. Kim, H.W. Kim, Hydroxyapatite layerings on titanium substrate with titania buffer layer processed by sol–gel method, Biomaterials 25 (2004) 2533–2538.
[18] S.T. Picraux, L.E. Pope, Tailored surface modification by ion implantation and laser treatment, Science 226 (1984) 615–622.
[19] E. György, A. Pérez Del Pino, P. Serra, J.L. Morenza, Chemical composition of dome-shaped structures grown on titanium by multi-pulse Nd:YAG laser irradiation, Appl. Surface Sci. 222 (2004) 415–422.
[20] H.M. Kim, F. Miyaji, T. Kokubo, T. Nakamura, Effect of heat treatment on apatite-forming ability of Ti metal induced by alkali treatment, J. Mater. Sci. Mater. Med. 8 (1997) 341–347.
[21] E. Landi, A. Tampieri, G. Celotti, R. Langenati, M. Sandri, M.S. Sprio, Nucleation of biomimetic apatite in synthetic body fluids: dense and porous scaffold development, Biomaterials 26 (2005) 2835–2845.
[22] C. Rey, Physico-chemical properties of nanocrystalline apatites: implications for biominerals and biomaterials, Mater. Sci. Eng. C 27 (2007) 198–205.
[23] H.E. Placko, S. Mishra, J.J. Weimer, L.C. Lucas, Surface characterization of titanium-based implant materials, Int. J. Oral. Maxillofac. Implants 15 (2000) 355–363.
[24] P. Trisi, R. Lazzara, A. Rebaudi, W. Rao, T. Testori, S.S. Porter, Bone-implant contact on machined and dual acid-etched surfaces after 2 months of healing in the human maxilla, J. Periodontol. 74 (2003) 945–956.
[25] J.L. Vossen, Thin Solid Films, Academic Press, San Diego, 1990, pp. 888.
[26] A.A. Campbell, Bioceramics for implant layerings, Mater. Today Nov. (2003) 26–31.
[27] T. Kokubo, Formation of biologically active bone-like apatite on metals and polymers by a biomimetic process, Thermochim. Acta 280 (1996) 479.
[28] A.H. Aparecida, Desenvolvimento de Estruturas Porosas de Polietileno de Ultra Alto Peso Molecular (PEUAPM) Recobertas com Apatitas para Substituição e Regeneração Óssea. Araraquara, 2009. 141p. Tese (Doutorado em Físico-Química) – Instituto de Química de Araraquara, Universidade Estadual Paulista.
[29] E. György, I.N. Mihailescu, P. Serra, A. Pérez del Pino, J.L. Morenza, Single pulse Nd:YAG laser irradiation of titanium: influence of laser intensity on surface morphology, Surf. Layer. Technol. 154 (2002) 63.
[30] D.D. Deligianni, N.D. Katsala, P.G. Koutsoukos, Y.F. Missirlis, Effect of surface roughness of hydroxyapatite on human bone marrow cell adhesion, proliferation, differentiation and detachment strength, Biomaterials 22 (2001) 87.
[31] C.J. Oss van, Interfacial Forces in Aqueous Media, Dekker, New York, 1994.
[32] Joint committee powder diffraction standard. Diffraction data base. Newton Square: International for Diffraction Data, 2005. 1 CD-ROM.
[33] R.A. Bini, M.L. Santos, E.A. Filho, R.F.C. Marques, A.C. Guastaldi, Apatite layerings onto titanium surfaces submitted to laser ablation with different energy densities, Surf. Coat. Technol. 204 (2009) 399–403.
[34] A. Pérez del Pino, P. Serra, J.L. Morenza, Oxidation of titanium through Nd:YAG laser Irradiation, Appl. Surf. Sci. 197–198 (2002) 887–890.
[35] J. Forsgren, F. Svahn, T. Jarmar, H. Engikvist, Formation and adhesion of biomimetic hydroxyapatite deposited on titanium substrates, Acta Biomater. 3 (2007) 980–984.
[36] H. Aoki, Science and Medical Applications of Hydroxyapatite, Takayama Press System Center, Tokyo, 1991, pp. 230.
[37] H.M. Kim, F. Miyaji, T. Kokubo, C. Ohtsuki, T. Nakamura, Bioactivity of Na_2O–CaO–SiO_2 glasses, J. Am. Ceram. Soc. 78 (1995) 2405.
[38] T. Nakazawa, Inorganic Phosphate materials, Elsevier, Tokyo, 1989, cap. 2, pp. 15.
[39] R.Z. Legeros, Properties of osteoconductive biomaterials: calcium phosphates, Clin. Orthop. Related Res. 395 (2002) 81.
[40] R.M. Silverstein, G.C. Bassler, T.C. Morril, Identificação espectrométrica de compostos orgânicos. 5. ed. Rio de Janeiro: Guanabara, 1994 pp.460.
[41] A. Stoch, W. Jastrzebski, A. Brozek, J. Stoch, J. Szaraniec, B. Trybalska, G. Kmita, FTIR absorption-reflection of biomimetic growth of phosphates on titanium implants, J. Mol. Struct. 555 (2000) 375.
[42] L.C.O. Vercik, Estudo do recobrimento de hidroxiapatita sobre superfície de Ti cp e liga Ti–6Al–4V, sem e com deposição de TiO2 por plasma-spray. 2004. 127 f. Tese (Doutorado em Química)–Instituto de Química, Universidade Estadual Paulista, Araraquara, 2004.
[43] W. Weng, J.L. Baptista, J sol–gel derived porous hydroxyapatite coatings, Mater. Sci. Mater. Med. 9 (1998) 159–163.
[44] S.W. Russel, K.A. Luptak, C.T.A. Suchiacital, T.L. Alford, V.B. Pizziconi, Sol–gel calcium phosphate ceramic coatings and method of making same, J. Am. Ceram. Soc. 79 (1996) 837–842.